International Forum on Aeroelasticity and Structural Dynamics
IFASD 2019
9-13 June 2019, Savannah, Georgia, USA

HIGH REYNOLDS NUMBER TESTING OF A LAMINAR AIRFOIL UNDER FORCED HARMONIC PITCHING OSCILLATIONS AT CRYOGENIC CONDITIONS

Holger Mai[1], Anne Hebler[1] and Stefan Koch[2]

[1] German Aerospace Center (DLR)
Institute of Aeroelasticity
Bunsenstraße 10, 37073 Göttingen, Germany
Holger.Mai@dlr.de
Anne.Hebler@dlr.de

[2] German Aerospace Center (DLR)
Institute of Aerodynamics and Flow Technology
Bunsenstraße 10, 37073 Göttingen, Germany
Stefan.Koch@dlr.de

Keywords: laminar airfoil, laminar-turbulent transition, flutter, unsteady aerodynamics, cryogenic wind tunnel, NLF-0415.

Abstract: Steady and unsteady aerodynamic testing of a pitching 2D laminar airfoil model was conducted at high Reynolds numbers under cryogenic conditions. The influence of the unsteady laminar-turbulent boundary layer transition on the aeroelastic stability and flutter behavior was investigated to assess the risk of applying this technology to transport aircraft.
In first tests the influence of free transition on a typical laminar CAST-10/2 airfoil on its aeroelastic stability could be derived. As the aim of the present test was to obtain unsteady aerodynamic data for an oscillating laminar airfoil in the high Reynolds number regime, a new hydraulic pitching mechanism was built that could be operated in an environment of low temperatures down to 100 K. Furthermore a new wind-tunnel model with NLF-0415 airfoil shape was built and equipped with unsteady pressure sensors, hot-film sensors and accelerometers. During the test systematic variations of the Mach number at constant Reynolds number and a variation of the Reynolds number at constant Mach number were performed. Steady lift and moment polars were recorded at Reynolds numbers of up to $14 \cdot 10^6$. As a first result, nonlinear behavior as already found for the CAST-10/2 airfoil in the transonic regime for low Reynolds numbers of $2 \cdot 10^6$, can also be found for the NLF-0415 airfoil for Reynolds numbers of up to $8 \cdot 10^6$.

1 INTRODUCTION

For modern transport aircraft operating in the transonic regime, drag reduction is expected to have the highest potential contributing to the challenging targets of ACAREs vision 2020 and Flightpath 2050 of reducing the fuel consumption and CO_2 emissions by 50% and NO_x by 80%. The potential of reduction of the friction drag on the whole aircraft by laminar flow on the wing is estimated to be about 11%. Nevertheless, the influence of this new technology on the aeroelastic behavior of the aircraft is still not sufficiently understood. It may change the flow characteristics significantly in contrast to modern supercritical transport aircraft wing

airfoils. Because of the altered shape of laminar wings, the thickness of the boundary layer and by that, the shock position may change and shock strength and dynamics may increase.
In principle, laminarization can be reached passively (natural laminar flow, NLF) by keeping the wing sweep angle moderate and by using laminar airfoils with a backward thickness maximum, actively with a boundary layer suction system or by a combination of both technologies which is then called hybrid laminar flow control, HLFC. Nevertheless, aircraft wings will always have a laminar-to-turbulent boundary layer transition.
In contrast to conventional (fully turbulent) airfoils, laminar airfoils show a distinct laminar bucket in the drag polar, because the flow can be kept laminar only for moderate angles of attack. At the border of the laminar drag bucket, the transition moves from the back of the airfoils surface in direction of the nose and by that induces a nonlinear effect on the local lift, which can be ascribed to the different increases of the displacement thickness of a laminar and a turbulent boundary layer.
Numerical aeroelastic methods are increasingly used as an alternative in certification to experimental proofs in wind tunnels and flight tests. This presumes that the CFD methods used have the required capabilities and are validated, especially in the boundary areas of the flight envelope. Before we had started our investigations there was a lack of validated transition and turbulence models for transonic, unsteady and transitional flows.
Therefore, steady and unsteady high fidelity computational fluid dynamics (CFD) calculations were performed for the CAST-10/2 airfoil in separate studies [1–3]. Reynolds-averaged Navier-Stokes (RANS) calculations combined with a γ-Reθ transition model were able to predict the laminar drag bucket as well as nonlinearities in the steady polars [4]. Differences in the unsteady airloads between turbulent and transitional flow were predicted by the simulations. The lower transonic dip for free transition, which was observed experimentally [5], was also found in the simulations, but in addition a shift towards lower Mach numbers was reported. Qualitatively, the results of the simulation and the experiment match, however quantitative differences existed. Flutter prediction for transitional flows can only work if the underlying transition models predict the drag bucket for stationary flows and at flight Reynolds numbers reliably [1]. Beyond, it has to be ensured that the dynamic behavior of the transition for a wing oscillating in its elastic modes can be described by an adequate, experimentally validated aerodynamic model.
Finally, a one-equation transition model was developed [6], using the experimental database from the former experiments. Only few data was available for the validation at high Reynolds numbers, therefore the experiment described in this paper can additionally provide valuable results.
Our former investigation [[7], [8]] showed that especially the unsteady dynamic behavior of the boundary layer and its interaction with transonic shocks is of great importance for aeroelastic stability and flutter. It may be expected that the so called transonic dip is more pronounced and buffeting already occurs at smaller transonic Mach numbers.
To clarify this, the processes that take place in the unsteady boundary layer of an oscillating airfoil have to be described in more detail. A good indicator for the activities in the boundary layer is the wall shear stress, as it changes for the different flow states. Experimentally the wall shear stress can be determined by using hot wire anemometry or hot-film sensors.
A systematic aeroelastic investigation for laminar wings is unknown in the literature. Numerical prediction tools for unsteady transition are still under development [9]. Therefore, DLR started a long-term strategy on the investigation of the influence of laminar-turbulent boundary layer transition on the aeroelastic stability.

2 STATE OF CURRENT RESEARCH

Since 2010 DLR performed several wind-tunnel tests focusing on the aeroelastic stability of a wing with extended laminar run length. The tests followed a long term strategy to reveal the influence of the unsteady laminar-turbulent boundary layer transition on the aeroelastic stability and flutter behavior and to assess the risk of applying this technology to transport aircraft [10]. In a step-by-step approach the investigation started with steady polars of a 2D airfoil section at low Reynolds numbers and will end in dynamic, high Reynolds number, transonic 3D wing tests. The target was to possibly discover new physical phenomena and to generate high quality data for the validation of unsteady transition models in CFD codes. First, steady results of lift polars of a CAST-10/2 airfoil were shown and their typical nonlinear appearance in the area of the laminar bucket was investigated (see Fig. 1) [11].

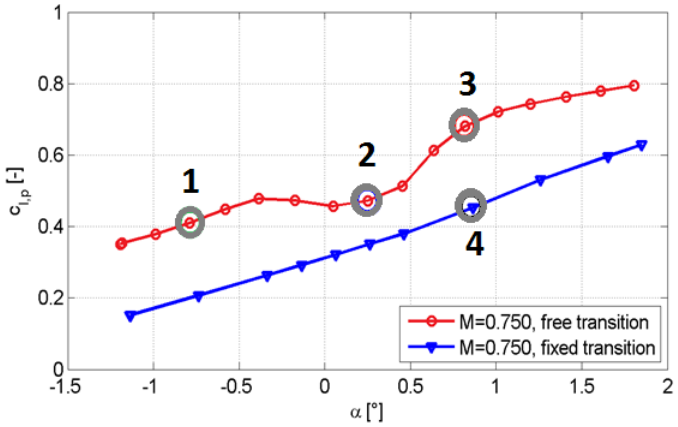

Figure 1: Steady lift polars for the CAST 10/2 airfoil at Re=2·106, Ma=0.75. [11].

The results were compared with the same airfoil undergoing turbulent flow, which was realized by fixing of the transition at x/c=0.075 on the pressure side and x/c=0.175 on the suction side of the wind-tunnel model with a strip of transition dots of 0.1270 mm height.
In [12] the impact of the steady nonlinear lift on the unsteady derivatives under harmonic pitching motion around particular points in the polar (marked 1, 2, 3 in Fig. 1) were investigated and used for a prediction of probable unstable points in a flutter setup [13]. In the follow-up flutter experiment [5] stability limits for fixed and free transition were investigated and different manifestations of limit cycle oscillations were found. From these results the influence of free transition on a typical laminar airfoil on its aeroelastic stability could be derived. Results for stable and unstable points in the total pressure over Mach number plane are plotted in Fig. 2. Stable points are marked with green symbols, unstable points are marked with red symbols. The stability limit around Mach 0.75 is called the transonic dip. It can be seen that for free transition the transonic dip is shifted to lower Mach numbers and its minimum is at lower total pressures.

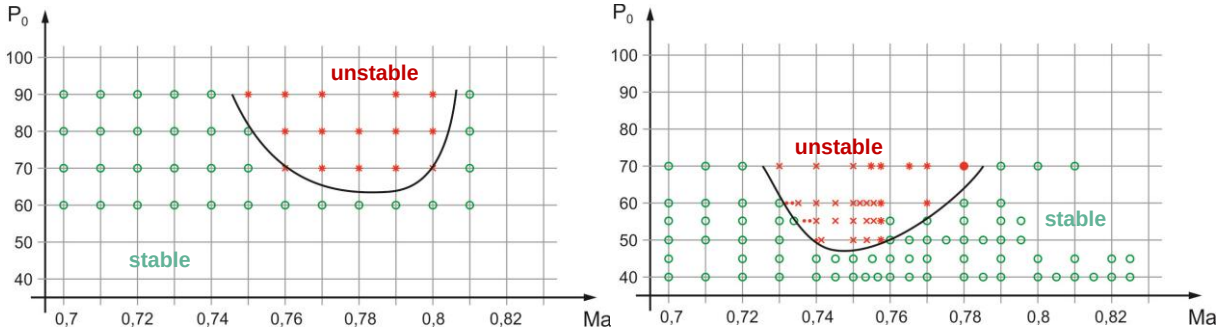

Figure 2: Stability limit for fixed (left) and free transition (right) for the CAST-10/2 airfoil at $Re=2\cdot10^6$.

As the results interfered with a laminar separation bubble (Fig. 7 in [12]), it was questioned whether the strong influence of the laminar-to-turbulent transition on the unsteady behavior is still present at higher, more realistic flight Reynolds numbers. In order to achieve such Reynolds numbers in the subsonic or transonic flight regime in a wind tunnel, either the chord length or the kinematic viscosity has to be changed. A scaling of the model is inapplicable, as a chord length of 3 m would be required, which is unsuitable for unsteady investigations. Therefore, the test was performed in the Cryogenic Wind-Tunnel Cologne (KKK). Here the kinematic viscosity can be changed by injecting nitrogen to cool down the working gas temperature to 100 K. This wind tunnel has the limitation that only subsonic wind speeds can be realized.
As the aim was to obtain unsteady aerodynamic data for an oscillating laminar airfoil in the high Reynolds number range, it was necessary to develop a new model suspension and excitation mechanism for model oscillations with variable frequencies and significant amplitudes under cryogenic conditions. Furthermore, a suitable airfoil that exhibits laminar flow at high Reynolds numbers had to be selected. It was a challenge to realize the construction of the wind-tunnel model, the instrumentation and the excitation mechanism for the unsteady motion of the model in the cryogenic environment. Therefore, a first focus of the paper will lie on the realization of the experiment under cryogenic conditions. Secondly, selected results of the measurements will be presented and conclusions regarding the aeroelastic behavior of the laminar airfoil at high Reynolds numbers will be drawn.

3 EXPERIMENTAL SET-UP

3.1 Model Geometry

For the wind-tunnel model the NLF-0415 airfoil was chosen. By MSES calculations it was assured that it shows significant laminar flow on the upper side of the airfoil up to Reynolds numbers of about $15 \cdot 10^6$. Calculations were also performed for several N-factors, as the actual turbulence level of the wind tunnel is unknown.

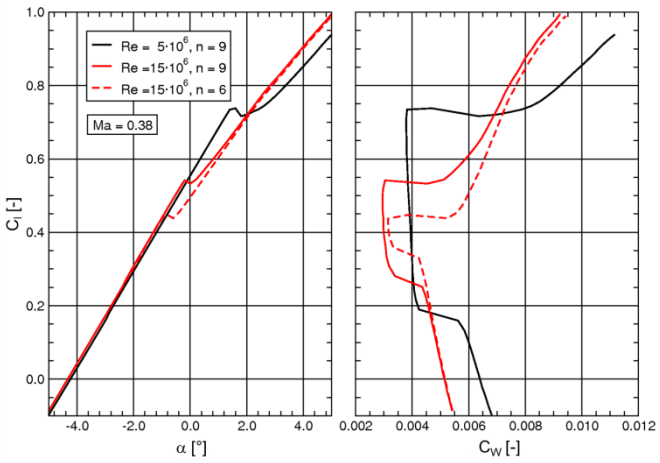

Figure 3: MSES calculations for different Reynolds numbers and N-factors.

The geometry was modified such that the trailing edge has a thickness of 1.46 mm in order to place a pressure sensor in the trailing edge.

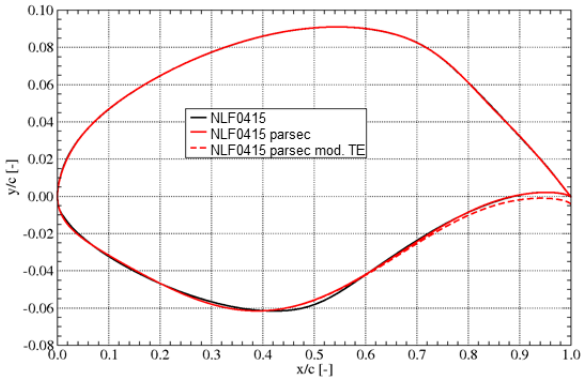

Figure 4: Modified NLF-0415 airfoil.

To be able to equip the model with all the instrumentation and to reduce weight and inertial moment, the model was designed and fabricated from carbon fiber reinforced plastic. As the 2D model had a span from wall to wall, it was necessary to clamp and drive the model on both sides. A special carbon fiber layout made it possible to reduce the temperature variation in span-wise direction below 0.1%. The model had a span of 2.4 m and a chord length of 0.4 m. The axis of rotation was 0.15 m in downstream direction at 37.5% chord length.
The model was mounted and excited on both sides by hydraulic torsional exciters. For that the model had root elements made of ASTM 579 steel laminated into the CFRP shells. The desired operational range is listed in Tab. 1. Within this operational range, four load cases were selected for the design and dimensioning of the carbon fiber layout.

Table 1: Operational range of the wind-tunnel model.

Angle of Attack	$-5° \leq \alpha_0 \leq +5°$
Amplitude	$0.02° \leq \alpha_{amp} \leq 1°$
Frequency	0.1 Hz – 26 Hz ($\alpha_{amp} \leq 1°$)
	0.1 Hz – 52 Hz ($\alpha_{amp} \leq 0.2°$)
Mach number	0.1 – 0.38
Reynolds number	$0.2 \cdot 10^6 – 15 \cdot 10^6$
Temperature	100 K – 300 K

3.2 Model instrumentation

The model was equipped with 75 differential unsteady pressure sensors of special type Kulite CCQ-132X-093-5D arranged in one central section on the upper and lower side of the airfoil to measure the unsteady pressure distribution (Fig. 5, green lines, Fig. 6). 65 hot-film sensors on three capton foils by TAO systems were applied to measure the unsteady boundary-layer transition (Fig. 5, blue rectangles). In order to measure the motion and deflection of the model, ten accelerometers of type PCB-351B41 with 100 mV/g sensitivity were installed in the model in five sections (Fig. 5, red dots). The temperature of the model was monitored using three PT-100 temperature sensors. Two additional temperature sensors were installed at each piezoelectric balance. The piezoelectric balances were installed between the hydraulic actuator and the model root on each side and used to measure the global forces and moments acting on the model. As the piezoelectric balances are not qualified for temperatures down to 100 K, they had to be kept in a constant temperature environment above 273 K.

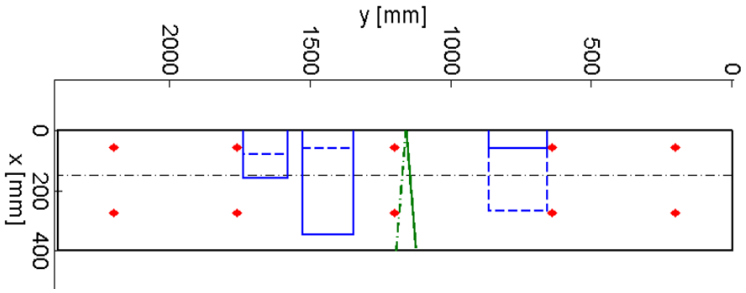

Figure 5: Position of sensors: Green marks the pressure orifices; blue the hot-film foils and red the accelerometer. Black dash-dotted line marks the axis of rotation.

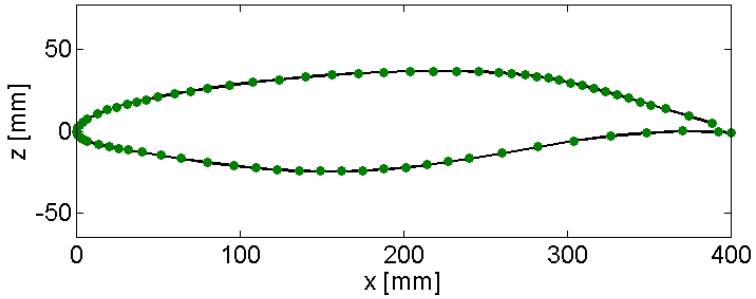

Figure 6: Detailed view on the distribution of the 75 unsteady pressure sensors.

3.3 Wind Tunnel and pitch oscillation test set-up

The Cryogenic Wind Tunnel Cologne (KKK) is operated by the foundation German-Dutch Windtunnels (DNW). The wind tunnel is a continuous run facility with a 2.4m x 2.4m test section (c.f. Fig. 7). The wind tunnel specifications are listed in Tab. 2. The ratio of the tunnel height to the chord length of the investigated airfoil model is 6.0. The side walls of the test section can be equipped with windows for model observation and optical measurement techniques. To prevent the windows from freezing up they are heated and in addition purged with hot gaseous nitrogen.

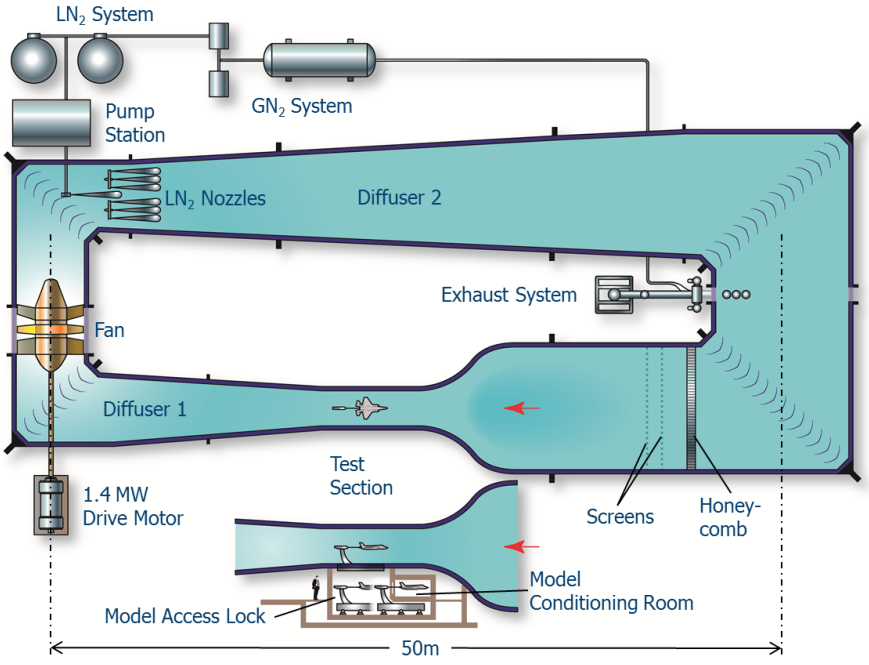

Figure 7: DNW-KKK Wind tunnel.

Table 2: Specification of KKK.

Test section size	2.4 m×2.4 m×5.4 m
Mach number	0.0 - 0.38
Reynolds number	0.4 Mio. – 40 Mio. (l_{ref}=1 m)
Stagnation pressure	atmospheric30 kPa – 150 kPa
Stagnation temperature	100 K – 300 K
Contraction ratio	10.4 : 1
Dynamic pressure	1 kPa

The model was mounted vertically in the test section of the wind tunnel (Fig. 8). On the upper and the lower side a bearing and a hydraulic actuator together with a piezoelectric balance were installed in an analogue way to [11] and [12]. As none of the hydraulic components including the tubes were temperature proof below 230 K, the whole set-up had to be capsuled and heated. In total 60 heating cartridges with a total power of 20 kW were installed to keep the piezoelectric balance, the bearings and the hydraulic system at ambient temperature.

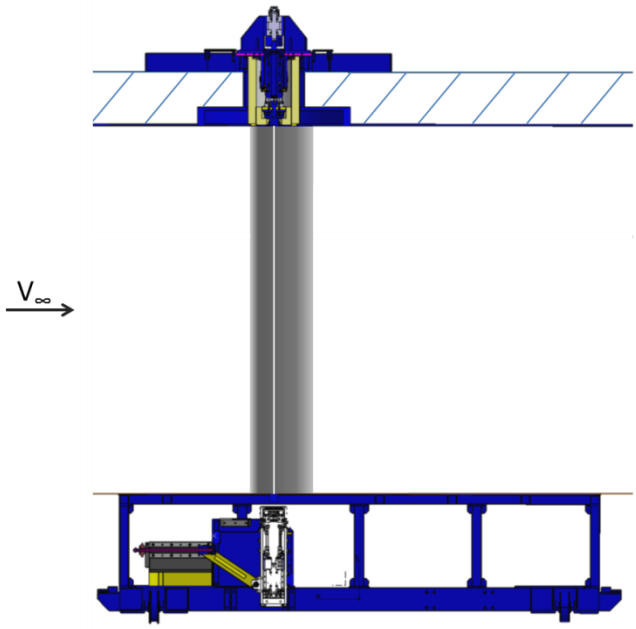

Figure 8: Pitch oscillation set-up.

It has been a special challenge to ensure sufficient stiffness of the set-up as both upper and lower hydraulics had to be mounted to the wind-tunnel walls with no additional frame in between (see Fig. 8).

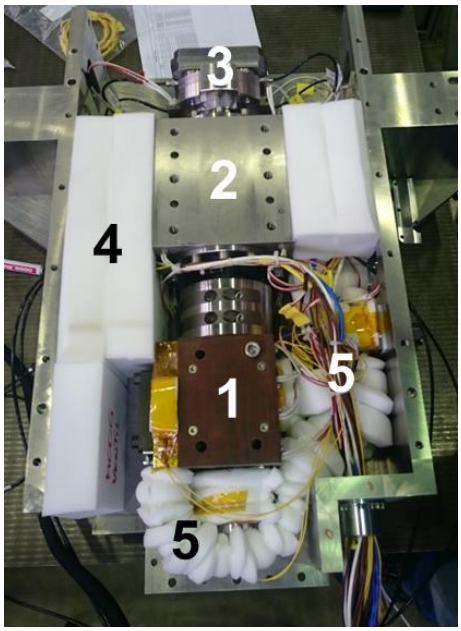

Figure 9: Detailed view on the lower hydraulics with hydraulic actuator (1), bearing (2), piezoelectric balance (3), isolation (5) and heating elements (5).

4 RESULTS

4.1 Steady lift- and moment polars

During the test systematic variations of the Mach number at constant Reynolds number and a variation of the Reynolds number at constant Mach number were performed. The main focus was on the Mach number of Ma = 0.340. Steady lift and moment polars between $-5° \leq \alpha_0 \leq +5°$ were recorded. As shown in Fig. 10 the polars exhibit similar nonlinearities as the CAST-10/2 airfoil.

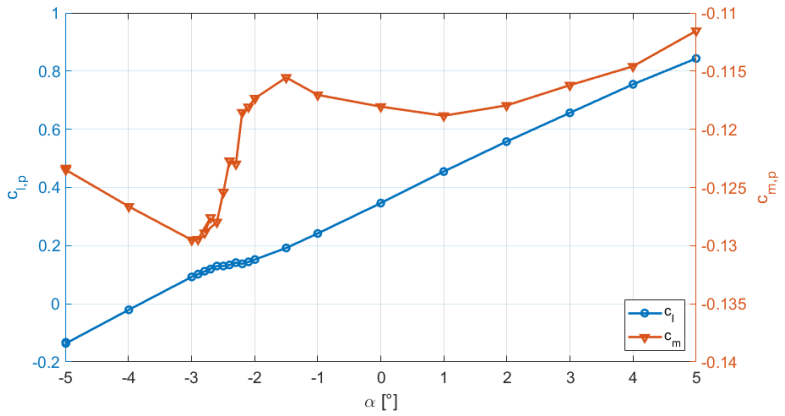

Figure 10: Steady lift and moment polar for the NLF0415 airfoil for Ma = 0.340 at Re = $6 \cdot 10^6$.

These nonlinearities can be connected with the abrupt change in drag at the upper end of the laminar drag bucket. This is shown in Fig. 11 for different Reynolds numbers.

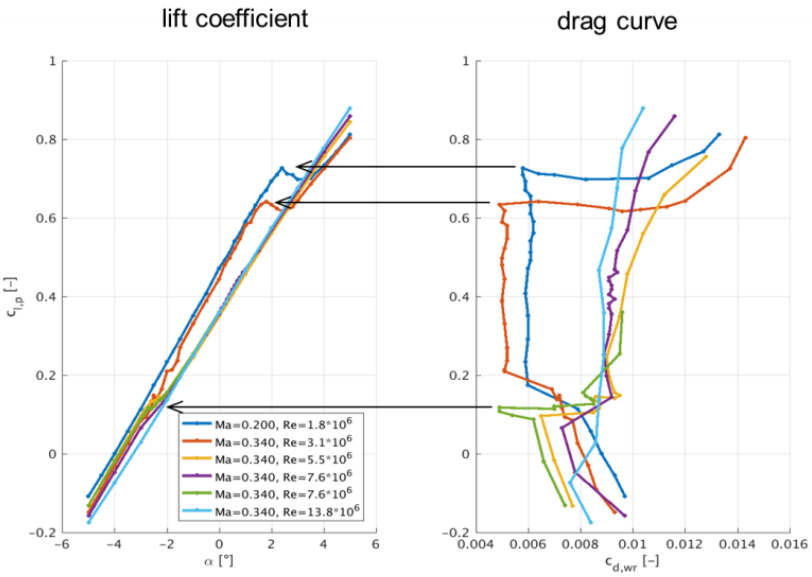

Figure 11: Steady lift and drag polars for the NLF0415 airfoil for Ma = 0.340 at different Reynolds numbers.

As the nonlinearity in the lift polar gets less pronounced with increasing Reynolds number, it becomes more difficult to detect. Observing the pitching moment, a descend of the momentum coefficient in the drag bucket and a steep increase right where the nonlinear lift has its first maximum can be identified (Fig. 10). By that, the nonlinearity can be identified more clearly in the development of the moment for the higher Reynolds numbers. This is presented in Fig. 12.

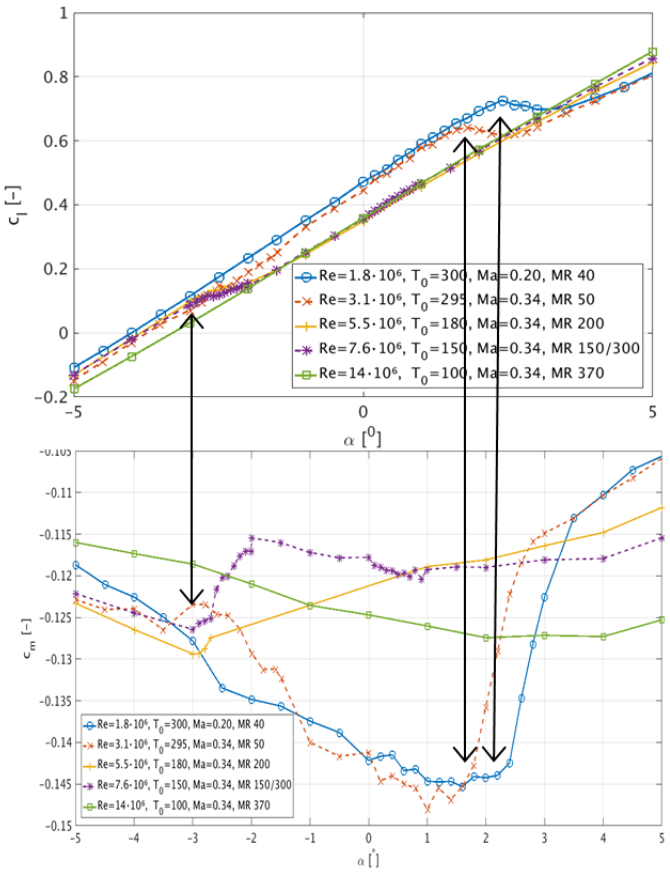

Figure 12: Steady lift and moment polars for the NLF0415 airfoil for Ma = 0.340 at different Reynolds numbers.

Also from that figure it is recognizable that for the highest Reynolds number of $14 \cdot 10^6$ the nonlinearity vanishes or at least cannot be detected anymore. This may be due to a change to turbulent flow as a result of deposits on the models surface at the time of this measurement or that the laminar drag bucket is too small or even not existent any more at that Reynolds number. This has to be the topic of further investigation.

4.2 Unsteady Results

In Fig. 13 to 15 results of transfer functions for variations of the oscillation frequency are presented. The different colors represent different mean angles of attack. Frequencies have been varied at a fixed oscillation amplitude of $\Delta\alpha = 0.2°$. Results for Reynolds numbers of 3.1, 5.9 and $13.3 \cdot 10^6$ are shown.

With reference to Fig. 12 it can be shown that for the lowest Reynolds number $3.1 \cdot 10^6$ the results at $\alpha_0 = 0.0°$ and $\alpha_0 = 3.0°$ presented in Fig. 13 are in the linear parts of the lift polar, whereas $\alpha_0 = 1.8°$ is at the local maximum in the nonlinear region and $\alpha_0 = 2.4°$ is in the minimum, respectively $\alpha_0 = 1.8°$ is at the minimum of the moment polar and $\alpha_0 = 2.4°$ at the ascending branch. The magnitudes of the lift derivatives in the nonlinear part (Fig. 13 a) are increasing with increasing frequency, whereas the magnitude of the lift derivative outside the nonlinear region is descending for $\alpha_0 = 0.0°$ in accordance with Theodorson's theory or nearly constant which is something in between the linear and the nonlinear region. The Phase (Fig. 13 b) for the latter two angles is slightly increasing whereas in the nonlinear region the phase has a distinct maximum. The magnitudes of the pitching moment derivatives (Fig. 13 c) show the same trend for all 4 angles of attack. However, the values of the points inside the nonlinearity are much higher. In the phase of the pitching moment derivative (Fig. 13 d) the smallest angle shows an increasing value starting at -180° as one would expect, whereas the other angles show nearly linear decreasing values starting at 0°.

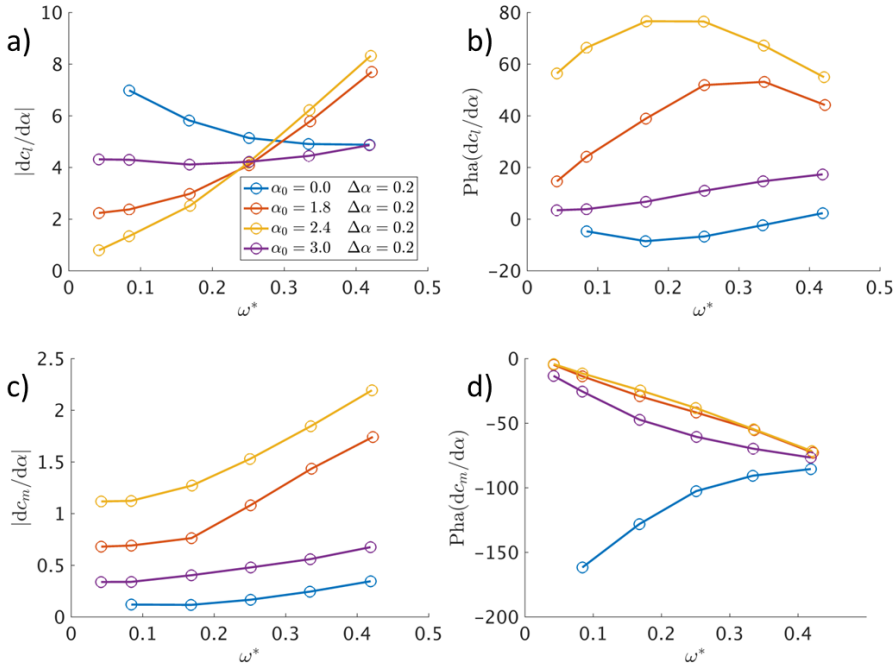

Figure 13: Magnitude and phase of unsteady lift and moment frequency variations for Ma = 0.340 at different mean α_0 for Re = $3.1 \cdot 10^6$.

For the middle Reynolds number of $5.9 \cdot 10^6$ the results presented in Fig. 14 look very similar for the different angles of attack. A presumption could be that although the mean angle of attack of $\alpha_0 = -2.7°$ is in the nonlinear region of the lift polar, the oscillation amplitude of $\Delta\alpha = 0.2°$ was so high and the nonlinear region so small that the oscillation extended to the linear part and was not much affected by the nonlinearity.

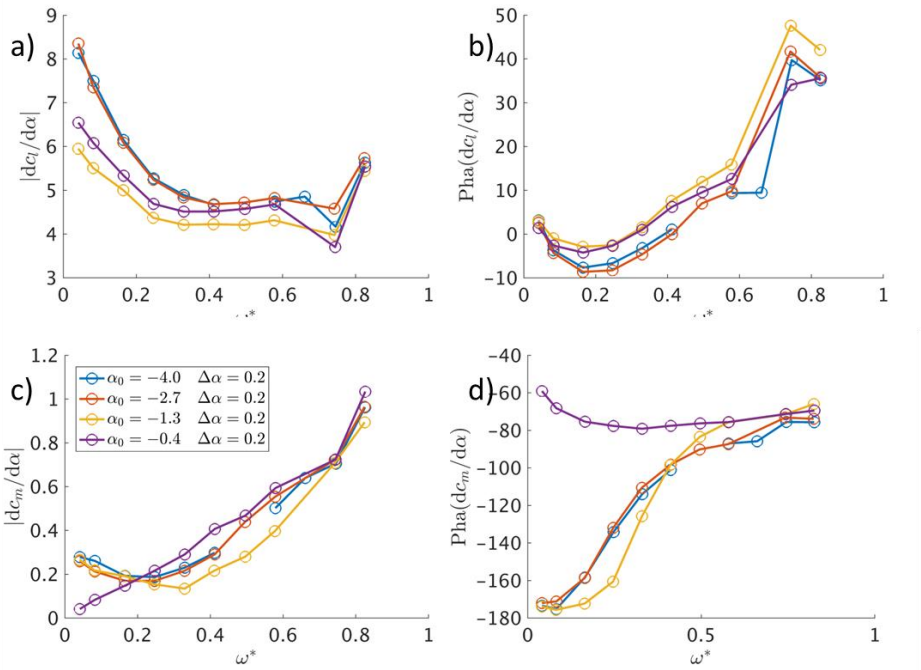

Figure 14: Magnitude and phase of unsteady lift and moment frequency variations for Ma = 0.340 at different mean α_0 for Re = $5.9 \cdot 10^6$.

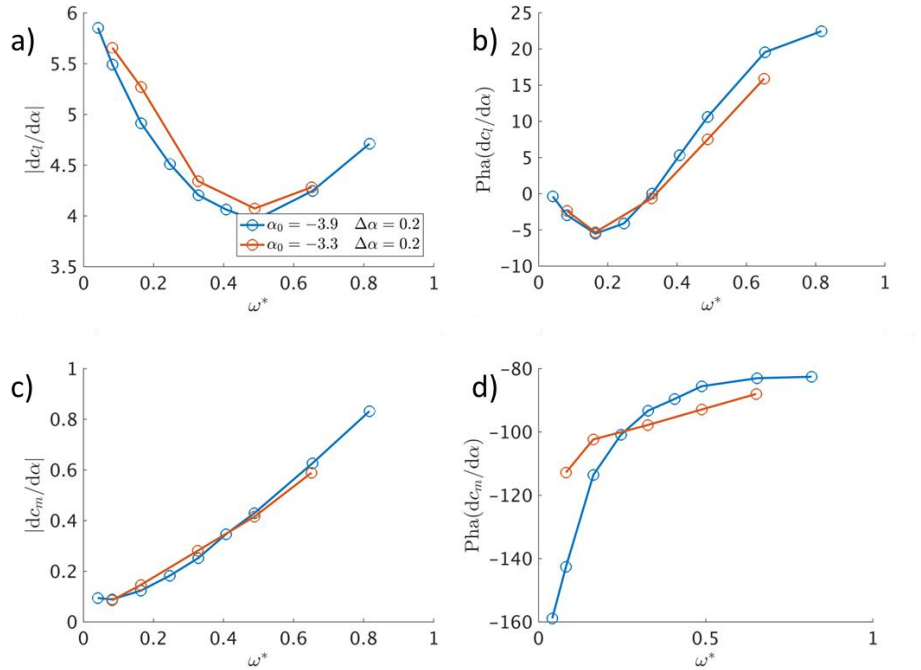

Figure 15: Magnitude and phase of unsteady lift and moment frequency variations for Ma = 0.340 at different mean α_0 for Re = $13.3 \cdot 10^6$.

For the highest Reynolds number of $13.3 \cdot 10^6$ the results for the magnitude of the unsteady lift coefficient (Fig. 15 a) show an interesting phenomenon: Starting at about 2π they are falling asymptotically down to a reduced frequency of $\omega^* = 0.5$. But from then on, they don't fall any further, they rise again, which contradicts Thodorson's theory.

4.3 Hot-Film Results

An exemplary result for the hot-film measurements is shown in Fig. 16. The airfoil model is performing a harmonic oscillation at a mean angle of attack of $\alpha_0 = 1.8°$ with an amplitude of $\Delta\alpha = 2°$. In the left plot the instantaneous α signal is plotted from bottom to top, in the right plot the time series of the sensors on the hot-film foil starting at the nose on the upper side of the airfoil model are shown. For each sensor its voltage signal is plottet with its zero value at the corresponding x/c position along the models chord. It can be seen that the transition is at x/c = 0.8 for the lowest angle of the oscillation and is moving in the direction of the models nose with increasing angle of attack. First slowly, then very suddenly the transition jumps forward and reaches its most forward position at 15% chord at the maximum angle of attack. It can be noticed that there is a small phase shift between the models α motion and the motion of the transition. In addition, the transition moves a little slower backwards than it moves forwards.

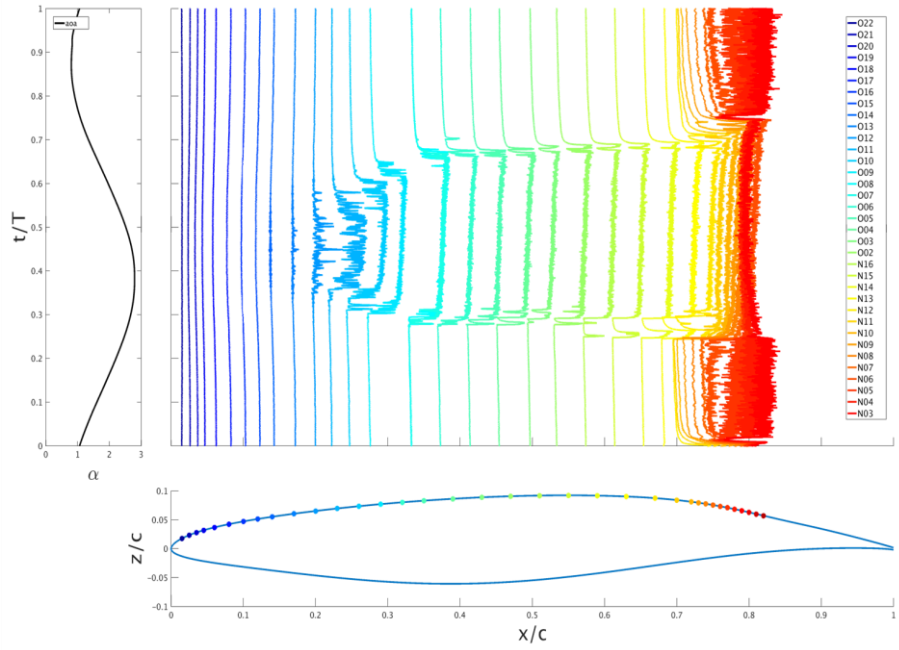

Figure 16: Hot film results for Ma = 0.340 at mean $\alpha_0 = 1.8°$ for $Re = 3.1 \cdot 10^6$.

5 SUMMARY

In its long term strategy DLR is investigating the influence of the unsteady laminar-turbulent boundary layer transition on the aeroelastic stability and flutter behavior of laminar airfoils. In the course of this steady and unsteady aerodynamic measurements have been performed at a pitching 2D airfoil model with laminar airfoil shape at high Reynolds numbers of up to $14 \cdot 10^6$ under cryogenic conditions. For the present test in a cryogenic wind tunnel, a new wind-tunnel model suitable for cryogenic conditions, instrumentation and a new hydraulic pitching mechanism have been built that could be operated at low temperatures of 100 K.

During the test systematic variations of the Mach number and the Reynolds number were performed. Steady lift and moment polars for mean angles of attack of $-5° \leq \alpha_0 \leq +5°$ were recorded. As a first result, the nonlinear behavior that has already been found for the CAST-10/2 airfoil in the transonic regime for low Reynolds numbers of $2 \cdot 10^6$, can also be found for the NLF-0415 supercritical laminar airfoil for Reynolds numbers up to $8 \cdot 10^6$. Whether the unsteady derivatives give an indication of possible unstable aeroelastic behavior will be part of further evaluation of the unsteady data.
Aeroelastic experiments of models undergoing significant amplitudes of motion at arbitrary frequencies at realistic flight Reynolds numbers are a challenge for the model, the instrumentation and the excitation system. The effort made to realize an aeroelastic test of a pitching airfoil undergoing harmonic pitch oscillations including the unsteady measurement techniques and the excitation apparatus all working at temperatures down to 100 K was very high. It could be shown, that the effort was worth it and according to DLRs strategy it was an important milestone on the way to an experiment with realistic Mach and Reynolds numbers in a larger transonic wind-tunnel facility that can represent high Reynolds numbers.

6 REFERENCES

[1] Fehrs, M., "Influence of Transitional Flow at Transonic Mach Numbers on the Flutter Speed of a Laminar Airfoil", Proceedings of the International Forum on Aeroelasticity and Structural Dynamics, IFASD 2013, Bristol, U.K. (2013)

[2] Fehrs, M., van Rooij, A. C. L. M., and Nitzsche, J., "Influence of Boundary Layer Transition on the Flutter Behavior of a Supercritical Airfoil", CEAS Aeronautical Journal, Vol. 6, No. 2 pp. 291–303. (2015)

[3] A. C. L. M. v. Rooij and W. Wegner, "Numerical investigation of the flutter behaviour of a laminar supercritical airfoil", In A. Dillmann et al., editors, New Results in Numerical and Experimental Fluid Mechanics IX, number 124 in Notes on Numerical Fluid Mechanics and Multidisciplinary Design, pages 3341. Springer International Publishing, Jan. 2014

[4] Fehrs, M., van Rooij, A.C.L.M. and Nitzsche, J., "Flutter Prediction in the transonic flight regime with the γ-Re_θ transition model", In: Proceedings of the 6th. European Conference on Computational Fluid Dynamics (ECFD VI), pp. 6334-6346, 20. - 25. Jul. 2014, Barcelona, Spain. ISBN 978-84-942844-7-2

[5] Hebler, A., "Experimental Assessment of the Flutter Stability of a Laminar Airfoil in Transonic Flow", Proceedings of the International Forum on Aeroelasticity and Structural Dynamics, IFASD 2017, Como, Italy (2017)

[6] Fehrs, M., "One-Equation Transition Model for Airfoil and Wing Aerodynamics", In: New Results in Numerical and Experimental Fluid Mechanics XI, pp. 199-208, ISBN 978-3-319-64518-6 (2016)

[7] Dietz, G., Schewe, G., Mai, H., „Experiments on Heave/Pitch Limit-Cycle Oscillations of a Supercritical Airfoil close to the Transonic Dip", Journal of Fluids and Structures Vol. 19, pp. 1-16 (2004)

[8] Dietz, G., Schewe, G., Mai, H., „Amplification and Amplitude Limitation of Heave/Pitch Limit-Cycle Oscillations Close to the Transonic Dip", Journal of Fluids and Structures Vol. 22, pp. 505-527 (2006)

[9] Krumbein A., Krimmelbein N., Schrauf G., "Automatic Transition Prediction for Three-Dimensional Aircraft Configurations using the DLR TAU Code", In: Notes on Numerical Fluid Mechanics and Multidisciplinary Design - New Results in Numerical

and Experimental Fluid Mechanics VII, Vol. 112. Springer Verlag, Berlin, Heidelberg. pp. 101-108. (2010)

[10] Tichy, L., Mai, H., Fehrs, M., Nitzsche, J., Hebler, A., "Risk Analysis for Flutter of Laminar Wings", Proceedings of the International Forum on Aeroelasticity and Structural Dynamics, IFASD 2017, Como, Italy (2017)

[11] Mai, H., Hebler, A., "Aeroelasticity of a Laminar Wing", Proceedings of the International Forum on Aeroelasticity and Structural Dynamics, IFASD 2011, Paris, France (2011)

[12] Hebler, A., Schojda, L., Mai, H., "Experimental Investigation of the Aeroelastic Behavior of a Laminar Airfoil in Transonic Flow", Proceedings of the International Forum on Aeroelasticity and Structural Dynamics, IFASD 2013, Bristol, England (2013)

[13] Hebler, A., Thormann, R., "Flutter Prediction of a Laminar Airfoil Using a Doublet Lattice Method Corrected by Experimental Data", In: New Results in Numerical and Experimental Fluid Mechanics X, pp. 445-455. Springer International Publishing, Switzerland (2016)

COPYRIGHT STATEMENT

The authors confirm that they, and/or their company or organization, hold copyright on all of the original material included in this paper. The authors also confirm that they have obtained permission, from the copyright holder of any third party material included in this paper, to publish it as part of their paper. The authors confirm that they give permission, or have obtained permission from the copyright holder of this paper, for the publication and distribution of this paper as part of the IFASD-2019 proceedings or as individual off-prints from the proceedings.